

A comment on comparing optimization on D-Wave and IBM quantum processors

Catherine C. McGeoch,¹ Kevin Chern,¹ Pau Farré,¹ and Andrew D. King^{1,*}

¹*D-Wave Quantum, Burnaby, British Columbia, Canada*

(Dated: June 28, 2024)

Recent work [1] presented an iterative hybrid quantum variational optimization algorithm designed by Q-CTRL and executed on IBM gate-based quantum processing units (QPUs), claiming a significant performance advantage against a D-Wave™ quantum annealer. Here we point out major methodological problems with this comparison. Using a simple unoptimized workflow for quantum annealing, we show success probabilities multiple orders of magnitude higher than those reported by Ref. [1]. These results, which can be reproduced using open-source code and free trial access to a D-Wave quantum annealer, contradict Q-CTRL’s claims of superior performance. We also provide a direct comparison between quantum annealing and a recent demonstration [2] of digitized quantum annealing on an IBM processor, showing that analog quantum annealing on a D-Wave QPU reaches far lower energies than digitized quantum annealing on an IBM QPU.

Among the proposed approaches for accelerating optimization with quantum computers, quantum annealing (QA) and the quantum approximate optimization algorithm (QAOA) have attracted the most interest. These approaches are run on annealing-based and gate-based quantum computers, respectively. QAOA has previously been compared against QA and random sampling [3–7].

One recent work from Q-CTRL [1] presents an iterative algorithm that is based on QAOA but which adds per-qubit angles $\theta_1, \dots, \theta_N$ that bias the initial qubit states during the iterative optimization. These angles θ_i play the role of linear-bias memory registers that are variationally tuned by the ansatz. Setting aside how these biases affect the computational role of quantum effects in this algorithm, we simply remark that the hybrid approach departs significantly from standard QAOA; to avoid confusion, we refer to the algorithm as “Q-CTRL”.

The matter we address here is the comparison, by Sachdeva *et al.* [1], between Q-CTRL and QA as implemented on a D-Wave quantum annealer. Ref. [1] claims significantly superior performance of Q-CTRL over QA, based on data taken from Pelofske *et al.* [3]. However, there are several major methodological problems with this comparison, which we now briefly list.

First, QA success probabilities are calculated using the sum total of all runs performed in an exploratory parametric grid search. The vast majority of the runs are obviously substandard *a priori*, and including them as serious problem-solving efforts results in much poorer statistical outcomes than would be produced by a basic, good-faith choice of parameters. No analogous parametric sweep was included in Q-CTRL’s reported results.

Second, success probabilities are used as the sole figure of merit, without comparing the time spent producing solutions. It is nonsensical to compare two algorithms with potentially vastly different runtimes using only success probability. For example, this would make it impossible to outperform brute-force algorithms. Time to solution

(TTS) is a widely used metric [8–11] that incorporates both runtime and success probability, and we use it here.

Third, classical postprocessing is applied, but only to Q-CTRL results. This obscures the computational role of the variational ansatz itself in the Q-CTRL results, and does not afford QA the same benefit of bitflip error correction.

Fourth, instead of running on an arguably unbiased set of six inputs, Ref. [1] compared Q-CTRL vs. QA using the three worst QA results from a 10-input testbed from Ref. [3], and three other auxiliary inputs also from Ref. [3] for which no QA results were published.

I. INPUT TYPES

Here we consider two types of optimization problems expressed in the classical Ising model of ± 1 spins.

Ref. [1] compares Q-CTRL and D-Wave on higher-order unconstrained binary optimization problems from Ref. [3], whose linear, quadratic, and cubic Ising energy terms are laid out in a 127-qubit “heavy-hex” geometry used by IBM gate-model processors. These inputs are specifically tailored to be amenable to both QAOA on IBM processors and QA on D-Wave Advantage™ processors. The cubic terms somewhat favor QAOA because in QA they must be order-reduced via the introduction of 138 slack variables in addition to the 127 spins in the system. We construct the instances and run the QA experiments as in Ref. [3], highlighting the fact that Q-CTRL’s claimed advantage disappears when standard and even-handed benchmarking methods are applied (Table I).

Ref. [1] also published results on weighted and unweighted max-cut problems. The unweighted problems are generated by NetworkX [12] with an explicit random seed, so we can run QA on these as well. Table I presents results from five such problems, named (N, d, s, u) where N , d , and s are the graph size, degree, and random seed, respectively, and “u” indicates an unweighted max-cut problem. Again, we will see that QA outperforms Q-CTRL.

* aking@dwavesys.com

Max-cut								
Global		Q-CTRL (IBM Quantum)			QA (D-Wave) Embedding time included			
Instance	Opt	P_{GS}	t_{sample} (ms)	TTS (ms)	P_{GS}	t_{sample} (ms)	TTS (ms)	
(28,3,102,u)	40	0.94	25	40	1	1.2	1.2	
(30,3,264,u)	43	0.92	25	46	1	1.2	1.2	
(32,3,7,u)	46	0.83	25	66	1	1.3	1.3	
(80,3,68,u)	106	0.14	28	868	0.23	1.6	28	
(100,3,12,u)	135	0.12	28	1000	0.53	1.6	9.5	
(120,3,8,u)	163	0.09	28	1436	0.79	1.6	4.6	

Higher-order spin glass								
Global		Q-CTRL (IBM Quantum)			QA (D-Wave)			
Instance	Opt	P_{GS}	t_{sample} (ms)	TTS (ms)	P_{GS}	t_{sample} (ms)	TTS (ms)	
0	-200	0.000134	28	962,210	0.002	0.21	488	
3	-198	0.12	28	1027	0.018	0.21	53	
5	-198	0.20	28	568	0.048	0.21	20	
10	-202	0.019	28	6651	0.135	0.21	6.7	
11	-180	0	28	∞	0.006	0.21	157	
69	-190	0	28	∞	0.009	0.21	110	

TABLE I. Comparison between Q-CTRL and QA on (top) unweighted max-cut and (bottom) higher-order spin-glass problems. Compare with Ref. [1] Table I. All D-Wave experiments are run on Advantage.System4.1 using 500 reads per programming and 1 ms annealing time. Higher-order spin-glass inputs are constructed as in Ref. [3], and use six parallel embeddings to draw six samples per read. To reduce uncertainty, QA experiments were repeated five times for each higher-order spin-glass input, yielding 15,000 samples, comparable to Q-CTRL experiments.

Additionally, we note that a better choice of gadgets than the one used in Ref. [3]¹ leads to significantly improved QA results (see Table II).

II. MAIN RESULTS

Instead of attempting to optimize QA parameters, we run QA on all inputs using 500 reads per QPU call, annealing time $t_a = 1$ ms, and all other parameters at default values. We run the same postprocessing on QA results as on Q-CTRL results, and we examine the effect of this postprocessing in the next section.

Table I summarizes our experimental results. To estimate Q-CTRL time per sample t_{sample} , we refer to Ref. [1] Appendix A, which specifies 6000 samples taking 150 seconds of QPU time for the three smallest inputs, and larger inputs taking 7 minutes for 15,000 samples; thus, 25 and 28 ms for these problem classes respectively.

Max-cut problems on random graphs cannot be assumed to fit directly into the Pegasus qubit connectivity graph of the D-Wave Advantage processor, so we heuristically minor-embed them using D-Wave’s Ocean™ software development kit [13], and include this overhead in the total runtime.

The higher-order spin-glass problems are specifically tailored to fit into both IBM and D-Wave hardware, and we use the same six parallel embeddings for all inputs. Thus QA yields 3000 samples for each 500-read QA call, and t_{sample} is less than the annealing time of 1 ms for these problems, even when QPU overhead is included.

Given that QA produces samples far faster than Q-CTRL, we compare the approaches on equal footing using the time-to-solution (TTS) metric, which estimates the time required to find a ground state with 99% probability. For a per-sample time t_{sample} and a ground-state probability P_{GS} ,

$$\text{TTS} = t_{\text{sample}} \cdot \max\left(\frac{\log(1 - 0.99)}{\log(1 - P_{GS})}, 1\right). \quad (1)$$

The max-cut inputs are easy enough to be solved with greedy descent: Ref. [1] reports that their “local solver” finds ground states for all such inputs; this local solver finds five local minima from a random initial state using greedy bitflips, and takes the best solution of the five as its output.

On all but two instances (Table I), QA shows better success probability than Q-CTRL. QA shows better time to solution (TTS) on all inputs, by a minimum of $30\times$.

III. EFFECT OF POSTPROCESSING

Ref. [1] shows Q-CTRL results without classical post-processing for only one input: max-cut (120,3,8,u). We

¹ This better choice simply replaces the upper gadget for energy penalty $d_{BAC} = -1$ in Ref. [3] Fig. 3 with the upper gadget for $d_{BA(-C)} = +1$.

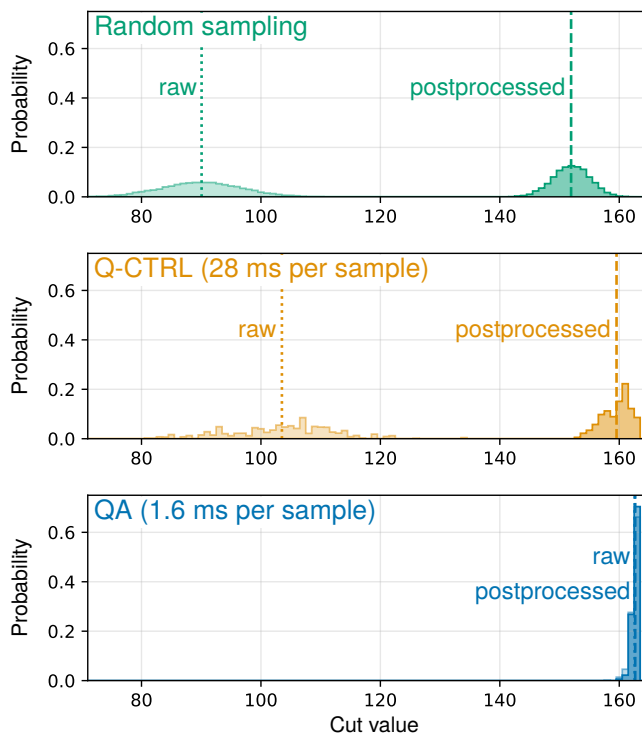


FIG. 1. Effect of postprocessing on max-cut instance (120,3,8,u). We show raw and postprocessed solution quality histograms for random sampling (top), Q-CTRL (middle) and QA (bottom). Dotted and dashed lines indicate raw and postprocessed mean values, respectively. Q-CTRL data and postprocessing method are taken from Ref. [1]. Optimal value of 163 was achieved by postprocessed Q-CTRL and both raw and postprocessed QA.

can therefore compare the effect of postprocessing on Q-CTRL and QA on this input. The postprocessing applied here sweeps through the spins in random order a maximum of five times, and flips a spin when it strictly improves the solution, thus finding a local minimum. Fig. 1 shows data for raw and postprocessed samples from random sampling, Q-CTRL, and QA. The data clearly shows that classical postprocessing is crucial to achieving good samples with Q-CTRL, and is far less important in QA.

Moving to the higher-order spin-glass problems, Table II compares raw and postprocessed ground-state probabilities for QA. We show the effect of postprocessing for both the original input construction of Pelofske *et al.* [3]—as considered in Ref. [1] and our Table I—and a modified construction in which the third gadget from [3] Fig. 3 is replaced by a version of the first gadget, with an appropriate spin-reversal transformation applied. This modification doubles the QA energy scale and significantly reduces the need for postprocessing. Forthcoming Advantage2™ systems have roughly a 2x relative boost to energy scales compared to the Advantage processors used here. An Advantage2 prototype is available online and can be used with free trial access to the Leap™ quantum

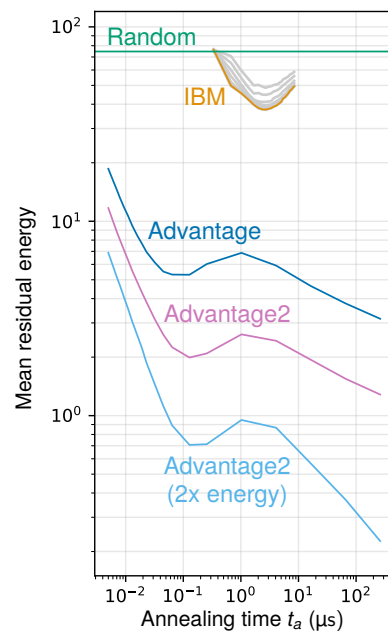


FIG. 2. Comparison of IBM and D-Wave processors on a 133-qubit heavy-hex spin-glass optimization problem. Residual energy (distance from optimal state) is shown as a function of annealing time. D-Wave Advantage system and Advantage2 prototype run analog quantum annealing; IBM Torino system runs digitized quantum annealing. Annealing times for IBM are based on an assumption of 4-gate depth per Trotter slice, with 84 ns gate time.

cloud service [14].

IV. COMPARING DIGITIZED AND ANALOG QA BETWEEN QUBIT MODALITIES

Recent work [2] evaluated the quality of gate-model quantum processors using digitized quantum annealing, within a framework of quantum critical dynamics. Similar evaluations have been demonstrated on D-Wave (analog) QA processors [15–18]. In particular, Ref. [2] demonstrated digitized QA on a 133-qubit heavy-hex spin glass. This planar spin glass has couplings J_{ij} distributed uniformly in $[-1, 1]$. This provides an opportunity to directly compare two quantum-computing modalities for optimization, with no hybrid methods, preprocessing, or postprocessing obscuring the contribution of the QPU. We show such a comparison in Fig. 2. Residual energies are much lower for QA, particularly for the Advantage2 prototype, owing to higher energy scale and lower noise.

We also test the effect of doubling energy scale in the Advantage2 prototype. Programmed couplings J_{ij} are constrained to the interval $[-2, 1]$, but this problem is small and sparse, and the couplings with $|J_{ij}| > 0.5$ induce a subgraph with no cycles. We can therefore find a spin-reversal transformation in linear time that compresses the spin-glass couplings to $[-1, 1/2]$ by flipping

Higher-order spin glass									
QA Construction from [3]					QA Better gadgets				
		P_{GS}		TTS (ms)		P_{GS}		TTS (ms)	
Inst.	raw	postprocessed	raw	postprocessed	raw	postprocessed	raw	postprocessed	
0	0.0005	0.002	1813	488	0.067	0.073	14	13	
3	0.005	0.018	193	53	0.22	0.24	4.0	3.6	
5	0.003	0.048	302	20	0.42	0.57	1.8	1.1	
10	0.087	0.135	11	6.7	0.58	0.61	1.1	1.0	
11	0.002	0.006	456	157	0.12	0.15	7.6	6.1	
69	0.002	0.009	483	110	0.07	0.08	13	11	

TABLE II. Effect of postprocessing on QA success probabilities and time to solution. Right-hand data (“better gadgets”) replaces the third gadget from Ref. [3] Fig. 3 with a spin-reversal transform of the first gadget. This doubles the QA energy scale, improving performance significantly and making postprocessing less impactful.

the sign of a subset of spin variables. This allows us to double the energy scale, leading to significantly smaller residual energies. This is informative but is not a method that generalizes well to large, dense problems.

Finally we remark that this spin-glass input is not computationally challenging, but these results shed light on the nature of quantum annealing in gate-model and annealing-based QPUs.

V. CONCLUSIONS

We have scrutinized recent claims [1] of gate-model optimization outperforming quantum annealing. These claims were founded on a benchmarking methodology that mistook poor-quality samples from a broad parameter sweep [3] for a good-faith effort to optimize efficiently, and ignored the cost of producing a sample, instead measuring only sample quality. Accounting for these issues, we found quantum annealing running on D-Wave processors to outperform Q-CTRL’s hybrid variational algo-

rithm running on IBM quantum processors. Our experiments can be repeated using free trial QPU access via D-Wave’s Leap cloud service [14].

We also compared solution quality on a planar spin-glass instance, and found that digitized quantum annealing running on IBM quantum processors is not competitive with analog quantum annealing running on D-Wave processors.

VI. CODE AVAILABILITY

Supporting data and code for running these experiments is available at Zenodo repository <https://doi.org/10.5281/zenodo.12549342>.

VII. ACKNOWLEDGMENTS

We are grateful to Elijah Pelofske, Alex Miessen and Guglielmo Mazzola for helpful discussions and providing experimental data.

-
- [1] N. Sachdeva, G. S. Harnett, S. Maity, S. Marsh, Y. Wang, A. Winick, R. Dougherty, D. Canuto, Y. Q. Chong, M. Hush, P. S. Mundada, C. D. B. Bentley, M. J. Biercuk, and Y. Baum, *Quantum optimization using a 127-qubit gate-model IBM quantum computer can outperform quantum annealers for nontrivial binary optimization problems* (2024), [arXiv:2406.01743](https://arxiv.org/abs/2406.01743).
- [2] A. Miessen, D. J. Egger, I. Tavernelli, and G. Mazzola, *Benchmarking digital quantum simulations and optimization above hundreds of qubits using quantum critical dynamics* (2024), [arXiv:2404.08053](https://arxiv.org/abs/2404.08053).
- [3] E. Pelofske, A. Bärtzchi, and S. Eidenbenz, Short-depth QAOA circuits and quantum annealing on higher-order ising models, *npj Quantum Information* **10**, 65 (2024).
- [4] M. Willsch, D. Willsch, F. Jin, H. De Raedt, and K. Michielsen, Benchmarking the quantum approximate optimization algorithm, *Quantum Information Process-*
ing **19**, 1 (2020).
- [5] E. Pelofske, J. Golden, A. Bartschi, D. O’Malley, and S. Eidenbenz, Sampling on NISQ Devices: “Who’s the Fairest One of All?”, *Proceedings - 2021 IEEE International Conference on Quantum Computing and Engineering, QCE 2021 I*, 207 (2021).
- [6] H. Ushijima-Mwesigwa, R. Shaydulin, C. F. Negre, S. M. Mniszewski, Y. Alexeev, and I. Safro, Multilevel Combinatorial Optimization across Quantum Architectures, *ACM Transactions on Quantum Computing* **2**, 10.1145/3425607 (2021).
- [7] M. P. Harrigan, K. J. Sung, M. Neeley, K. J. Satzinger, F. Arute, *et al.*, Quantum approximate optimization of non-planar graph problems on a planar superconducting processor, *Nature Physics* **17**, 332 (2021).
- [8] T. F. Rønnow, Z. Wang, J. Job, S. Boixo, S. V. Isakov, D. Wecker, J. M. Martinis, D. A. Lidar, and M. Troyer,

- Defining and detecting quantum speedup, *Science* **345**, 420 (2014).
- [9] T. Albash and D. A. Lidar, Adiabatic quantum computation, *Reviews of Modern Physics* **90**, 015002 (2018).
- [10] M. Cain, S. Chattopadhyay, J.-G. Liu, R. Samajdar, H. Pichler, and M. D. Lukin, Quantum speedup for combinatorial optimization with flat energy landscapes (2023), [arXiv:2306.13123](https://arxiv.org/abs/2306.13123).
- [11] H. M. Bauza and D. A. Lidar, Scaling Advantage in Approximate Optimization with Quantum Annealing (2024), [arXiv:2401.07184](https://arxiv.org/abs/2401.07184).
- [12] NetworkX, <https://networkx.org/>.
- [13] Ocean Developer Tools, <https://docs.ocean.dwavesys.com>.
- [14] The Leap Quantum Cloud Service, <https://www.dwavesys.com/solutions-and-products/cloud-platform/>.
- [15] Y. Bando, Y. Susa, H. Oshiyama, N. Shibata, M. Ohzeki, F. J. Gómez-Ruiz, D. A. Lidar, S. Suzuki, A. del Campo, and H. Nishimori, Probing the universality of topological defect formation in a quantum annealer: Kibble-Zurek mechanism and beyond, *Physical Review Research* **2**, 033369 (2020).
- [16] A. D. King, S. Suzuki, J. Raymond, A. Zucca, T. Lanting, *et al.*, Coherent quantum annealing in a programmable 2,000 qubit Ising chain, *Nature Physics* **18**, 1324 (2022).
- [17] A. D. King, J. Raymond, T. Lanting, R. Harris, A. Zucca, *et al.*, Quantum critical dynamics in a 5,000-qubit programmable spin glass, *Nature* **617**, 61 (2023).
- [18] M. H. Amin, A. D. King, J. Raymond, R. Harris, W. Bernoudy, *et al.*, Quantum error mitigation in quantum annealing (2023), [arXiv:2311.01306](https://arxiv.org/abs/2311.01306).